Scaling properties of a model for ruptures in an elastic medium

1997 J. Phys. A: Math. Gen. 30 3407

(http://iopscience.iop.org/0305-4470/30/10/018)

J. Phys. A: Math. Gen. **30** (1997) 3407–3419. Printed in the UK PII: S0305-4470(97)76430-8

Scaling properties of a model for ruptures in an elastic medium

Daniel Groleau†, Birger Bergersen† and Huang-Jian Xu‡

† Department of Physics and Astronomy, University of British Columbia, Vancouver, BC, Canada, V6T 1Z1

‡ Department of Physics, University of Manitoba, Winnipeg, MB, Canada, R3T 2N2

Received 12 July 1996, in final form 11 February 1997

Abstract. We generalize a model proposed by Xu *et al* for ruptures in an elastic medium subject to shear stress. This model is applied to the study of earthquakes. We restrict ourselves to one-dimensional discretizations of the region on which we focus and consider the effects of disorder, degree of stress release and degree of stress nonconservation (dissipation). The one-dimensional systems display power-law cumulative size–frequency distributions over a certain range of size. The power laws cut off due to finite-size effects, i.e. the effects of the finite size of the system and the finite size of the basic unit of discretization. In addition, in the absence of disorder, there is a crossover region at small sizes and its origin is explained. The scaling properties in the absence of dissipation are characterized by exponents τ and ν as well as by a function f dependent on the parameters of the model. τ is associated with the cumulative size–frequency distribution in the thermodynamic limit, ν with the finite size of the system and f with the finite size of the basic unit of discretization. When stress dissipation is introduced into the model, a characteristic earthquake size smaller than system size appears, in contrast with the case in which stress dissipation is absent.

1. Introduction

A number of dynamical systems with many degrees of freedom reach a critical state without parameter fine-tuning. This phenomenon is commonly referred to as self-organized criticality (SOC) [1] and is characterized by power-law behaviour (scale invariance) in the thermodynamic limit. As pointed out by Sornette *et al* [2], many systems exhibiting SOC can be mapped onto equivalent equilibrium systems exhibiting a continuous phase transition. The absence of need for fine tuning of the parameter(s) arises because the system is driven so that the order parameter takes on an infinitesimally small positive value, forcing the system to be in the critical fluctuation regime. Finite-size scaling has proven immensely successful in the study of ordinary critical phenomena. The analogy with SOC suggests that the technique might be useful in analysing self-organized critical phenomena as well.

Bak and Tang [3] as well as Sornette and Sornette [4] were among the first to propose that the concept of SOC applies to earthquakes. Sornette and Sornette [4] argued that the structure of the earth's crust could be viewed as resulting from a SOC phenomenon. Bak and Tang [3] and Bak and Chen [5] demonstrated that simple stick-slip (short-range) conservative models, similar to a model that had been proposed for earthquakes [6], evolve to a self-organized critical state. However, in real earthquakes, fracture as well as friction are two equally important processes. Fracture occurs when the earth's crust yields as shear stress builds up from the grinding of tectonic plates against each other. Friction controls the

0305-4470/97/103407+13$19.50

subsequent slipping along the faults formed. It is of interest to note that the incorporation of fracture and friction in a unique model is a formidable task which is beyond the scope of the present paper (however, see [7]).

In other models [8–10], only fracture is considered. These models, which have long-range stress redistribution, are based on a continuum description of matter, and they have many features in common with models presented in the context of the fracture of materials [11]. The main difference between the above long-range models is that in [8] a dipole source term is employed, while the correct double couple representation of the earthquake source [12] is used in [9, 10]. The model of Xu *et al* [9, 10] is the one on which we will focus in this work.

The mathematical structure of the model of Xu *et al* is related to the ones proposed by Olami *et al* [13] and Lise and Jensen [14]. It is also related to integrate-and-fire models for pulse-coupled oscillators [15, 16]. The model of Xu *et al* is different from the ones quoted above in that a double couple source gives rise to long-range interactions, whereas [13] only considers nearest neighbours, and [14] treats a situation where a relaxing element interacts with a small number of randomly selected other elements. Integrate-and-fire models usually assume interactions where the relaxing *stress* is either distributed equally to all the other elements of the system [15] or short-range interactions [16], unlike elastic stress which is long-range but falls off with distance. As we shall see, these differences are significant.

The aim of this paper is to study the scaling properties of the model of Xu *et al* [9, 10]. We consider one-dimensional discretizations and study the effects of disorder, degree of stress release and degree of stress nonconservation (dissipation). The use of one-dimensional lattices allows us to go to large lattice sizes, and to check if the scaling laws are valid over the whole range of lattice sizes. Our motivation is that due to finite-size effects, the system is never completely scale invariant. It is therefore important to sort out effects due to the finite size of the system, and those due to the finite size of the basic unit of discretization. This problem arises because systems of interest are heterogeneous on scales much smaller than the discretization unit, so that the continuum limit is not meaningful. Quantities relating to stress threshold, degree of stress release and degree of stress dissipation may therefore be dependent upon the size of the discretization unit and the size of the system in a non-trivial way. This type of dependence was realized by Weibull in his pioneering work [17], but has since often been forgotten.

The organization of this paper is as follows. In section 2 we present a version of the model of Xu *et al* along with a new ingredient to it (coarse-graining of the lattice Green function used in the calculation of stress redistribution upon rupture). In section 3, we apply this version of the model to the study of earthquakes and present our results in section 4. Finally, we summarize these results and draw our conclusions in section 5.

2. The model

The model of Xu *et al* [9, 10] focuses on a planar region embedded in an infinite medium, neglecting the effect of any activity originating outside the region (open boundary conditions). The region of interest is divided into $L_1 \times L_2$ square units with the lattice constant, a, taken to be unity. A displacement vector is defined on each node (corner of a square) and the distortion of a unit is characterized by the strain tensor, u, which is defined at its centre. Initially, all deformations are elastic and the stress tensor, $\boldsymbol{\sigma}$, is related to the strain tensor through the special Hooke's law:

$$\sigma_{ij}(\boldsymbol{r}) = \lambda' \delta_{ij} u_{ll}(\boldsymbol{r}) + 2\mu u_{ij}(\boldsymbol{r})$$

where μ is the shear modulus, and λ' a Lamé constant modified to take into account the plane-stress geometry of the problem (see [18] for instance). Summation over repeated indices ($i, j = x, y$) is implied.

In the quiescent periods, the force balance condition $D_j\sigma_{ij} = 0$ must be satisfied on each square, where $D_{x,y}$ are the discrete derivatives, defined respectively as

$$D_x g(\boldsymbol{r}) \equiv \frac{1}{2}\left[g\left(\boldsymbol{r} + \frac{\hat{\boldsymbol{x}} + \hat{\boldsymbol{y}}}{2}\right) + g\left(\boldsymbol{r} + \frac{\hat{\boldsymbol{x}} - \hat{\boldsymbol{y}}}{2}\right) - g\left(\boldsymbol{r} - \frac{\hat{\boldsymbol{x}} + \hat{\boldsymbol{y}}}{2}\right) - g\left(\boldsymbol{r} - \frac{\hat{\boldsymbol{x}} - \hat{\boldsymbol{y}}}{2}\right)\right]$$

and

$$D_y g(\boldsymbol{r}) \equiv \frac{1}{2}\left[g\left(\boldsymbol{r} + \frac{\hat{\boldsymbol{x}} + \hat{\boldsymbol{y}}}{2}\right) - g\left(\boldsymbol{r} + \frac{\hat{\boldsymbol{x}} - \hat{\boldsymbol{y}}}{2}\right) - g\left(\boldsymbol{r} - \frac{\hat{\boldsymbol{x}} + \hat{\boldsymbol{y}}}{2}\right) + g\left(\boldsymbol{r} - \frac{\hat{\boldsymbol{x}} - \hat{\boldsymbol{y}}}{2}\right)\right]$$

when acting on the arbitrary function $g(\boldsymbol{r})$, where $\hat{\boldsymbol{x}}$ and $\hat{\boldsymbol{y}}$ are unit vectors oriented along the X-axis and Y-axis respectively. Now, assume that a rupture occurs at the square centred at $\boldsymbol{r}_0$. We consider only one shear mode of rupture, which occurs when shear stress σ_{xy} at $\boldsymbol{r}_0$ exceeds the stress threshold at that square. The additional shear stresses (σ'_{ij}) caused by the rupture are separated into an elastic part (σ^{el}_{ij}) and a non-elastic part (at $\boldsymbol{r}_0$ only). The new stress tensor components can then be expressed as

$$\sigma^{\text{new}}_{ij}(\boldsymbol{r}) = \sigma^{\text{old}}_{ij}(\boldsymbol{r}) + \sigma'_{ij}(\boldsymbol{r})$$

where

$$\sigma'_{xy}(\boldsymbol{r}) = \sigma^{el}_{xy}(\boldsymbol{r}) - f\sqrt{2}\delta_{\boldsymbol{r},\boldsymbol{r}_0} \tag{1}$$

$$\sigma'_{xx}(\boldsymbol{r}) = \sigma^{el}_{xx}(\boldsymbol{r}) \tag{2}$$

$$\sigma'_{yy}(\boldsymbol{r}) = \sigma^{el}_{yy}(\boldsymbol{r}). \tag{3}$$

At equilibrium, $\sigma^{\text{new}}_{ij}(\boldsymbol{r})$ must also satisfy the force balance condition on each square and as a result,

$$D_j\sigma'_{ij} = 0 \tag{4}$$

since $D_j\sigma^{\text{old}}_{ij} = 0$. Using (1)–(3) in (4), it can be shown [10] that

$$D_j\sigma^{el}_{ij} + F^d_i = 0$$

where

$$F^d_x = \frac{f}{\sqrt{2}}[\delta_{\boldsymbol{r},\boldsymbol{r}_0+\frac{\hat{x}+\hat{y}}{2}} - \delta_{\boldsymbol{r},\boldsymbol{r}_0+\frac{\hat{x}-\hat{y}}{2}} - \delta_{\boldsymbol{r},\boldsymbol{r}_0-\frac{\hat{x}+\hat{y}}{2}} + \delta_{\boldsymbol{r},\boldsymbol{r}_0-\frac{\hat{x}-\hat{y}}{2}}]$$

and

$$F^d_y = \frac{f}{\sqrt{2}}[\delta_{\boldsymbol{r},\boldsymbol{r}_0+\frac{\hat{x}+\hat{y}}{2}} - \delta_{\boldsymbol{r},\boldsymbol{r}_0-\frac{\hat{x}+\hat{y}}{2}} - \delta_{\boldsymbol{r},\boldsymbol{r}_0-\frac{\hat{x}-\hat{y}}{2}} + \delta_{\boldsymbol{r},\boldsymbol{r}_0+\frac{\hat{x}-\hat{y}}{2}}].$$

Therefore, σ^{el}_{ij} can be viewed as being generated by the external source $\boldsymbol{F}^d = (F^d_x, F^d_y)$, which is only non-zero at the corners of the ruptured unit, and is shown in figure 1(a) of [10]. $\boldsymbol{F}^d$ satisfies the conditions that its net force and net torque are zero, and thus is a double couple [12] (a term used in seismology to describe the earthquake source). f is the double couple force.

Next, $\sigma^{el}_{ij}(\boldsymbol{r})$ can be determined by using the above earthquake source and the method of Fourier transformation. Since $\sigma^{el}_{xy}(\boldsymbol{r})$ is the *only relevant* component of the stress tensor, we drop the subscript (from now on, stress simply refers to the shear stress component σ_{xy}). It can be shown [10] that the redistributed field is given by

$$\sigma'(\boldsymbol{r}) \equiv \sigma'_{xy}(\boldsymbol{r}) = -\tilde{f}G(\boldsymbol{r} - \boldsymbol{r}_0) \tag{5}$$

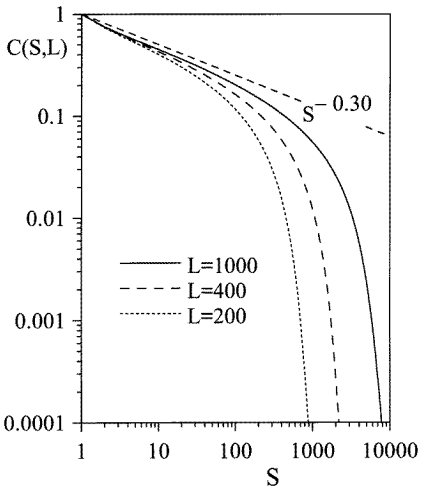

Figure 1. Log–log plot of the cumulative size–frequency distributions for $L \times 1$ lattices, random σ_{th}, $X = 0$, $\theta_l = 0.25$ and $\alpha = 1$. For comparison, we show the curve $C(S) = S^{-0.30}$.

where $\tilde{f} = f\sqrt{2}(\lambda' + \mu)/(\lambda' + 2\mu)$ and G is a lattice Green function expressed as

$$G(\boldsymbol{r}) = \int_{-\pi}^{\pi} \frac{\mathrm{d}k_x}{2\pi} \int_{-\pi}^{\pi} \frac{\mathrm{d}k_y}{2\pi} \frac{\sin^2 k_x \sin^2 k_y}{(1 - \cos k_x \cos k_y)^2} \mathrm{e}^{\mathrm{i}\boldsymbol{k}\cdot\boldsymbol{r}}. \tag{6}$$

In the model, the unit of discretization may be sufficiently large that the whole unit will not break in an individual rupture event. Instead, it will retain some shear stress. Assuming that

$$\sigma^{\mathrm{new}}(\boldsymbol{r}_0) = X\sigma^{\mathrm{old}}(\boldsymbol{r}_0)$$

where X is the fraction of the original stress which is not released, (5) can be rewritten as

$$\sigma'(\boldsymbol{r}) = -(1 - X)\sigma^{\mathrm{old}}(\boldsymbol{r}_0)G(\boldsymbol{r} - \boldsymbol{r}_0)/G(\boldsymbol{0}). \tag{7}$$

The case $X = 0$ corresponds to a rupture opening the whole element, as in [19]. The interpretation of a rupture event and the scaling properties are somewhat different if $X \neq 0$. We expect that parameter X and the stress threshold distribution depend on the size of the discretization unit. In fact, we can consider two discretizations of the same system, one with a coarser mesh than the other. Then, a coarser mesh element ruptures more often than a finer mesh element, but the total number of rupture events in the whole system is the same. We will come back to these considerations below.

Often, a necessary condition for SOC is the existence of a conservation law [20] (stress conservation in the present model). However, SOC has also been found in models with apparently no such law [13, 21, 22]. Stress dissipation can be incorporated into the model by multiplying $\sigma'(\boldsymbol{r})$ in (7) at all $\boldsymbol{r}$ except $\boldsymbol{r}_0$ by a factor α between 0.0 and 1.0. The effect of α is to make a fraction of the stress disappear from the system during redistribution. In addition, there is some stress which is redistributed outside the active region. The latter fraction goes to zero in the limit where the size of the active region goes to infinity. In all cases, the system organizes itself into a stationary state where on average the stress build-up balances the stress which is removed from the active region.

After the original rupture at $\boldsymbol{r}_0$, which is followed by stress redistribution, it can happen that the stress exceeds the stress threshold on several squares. We will then let them all break independently and add the respective stress redistribution contributions. This procedure was used as well in [8–10]. Other rules for the order in which the squares break might have also been considered. For instance, we could have picked only the square whose stress

exceeds its stress threshold most. We could, as well, have considered a self-consistent scheme in which the redistributed stresses from different broken squares are coupled [19]. The problem of describing what happens during the short period when the system is out of equilibrium during a rupture event is a difficult one (see [23]). We employ the independent rupture procedure because it is the simplest.

2.1. Coarse-graining of the lattice Green function

The lattice constant (a) has been chosen to be unity, so the coordinates of $\boldsymbol{r} - \boldsymbol{r}_0$ in (7) can be expressed as the set of integers (I, J). It is easy to verify that the lattice Green function (6) vanishes when $I+J$ is odd and is non-zero for $I+J$ even. This unphysical property can be overcome by a coarse-graining procedure.

We consider first a one-dimensional strip having $2L_1$ units. We imagine that one of the elementary units (the source unit) breaks. During the redistribution which follows, we mentally combine the units pairwise, so that there are now L_1 pairs of units in the lattice. The lattice Green function associated with the pairs can be expressed as

$$\bar{G}^1(I, 0) = G(2I, 0)$$

where $2I$ is the distance between the left(right) source unit to a given left(right) unit (in unit of a), and $I = 0, 1, 2, \ldots, L_1 - 1$ is the distance between the pairs (in unit of $2a$). Note that G can be multiplied by a global constant without changing the redistributed stresses [see (7)]. $G(I, 0)$ (I even) is a smooth function of I which falls off approximately as $1/I^2$ at large I.

For completeness, it can be mentioned that in the case of a two-dimensional $(2L_1) \times (2L_2)$ lattice of squares having $a = 1$, we can, during the redistribution which follows the rupture of an elementary unit (source unit), generalize the above procedure by mentally combining four of them such as to form a bigger square unit with lattice constant $a = 2$. The lattice now has $L_1 \times L_2$ units with $a = 2$. The most natural coarse-grained lattice Green function can be expressed as

$$\bar{G}^2(I, J) = G(2I, 2J) + \tfrac{1}{4}[G(2I + 1, 2J + 1) + G(2I + 1, 2J - 1) + G(2I - 1, 2J + 1) + G(2I - 1, 2J - 1)]$$

where $I = 0, 1, 2, \ldots, L_1 - 1$ and $J = 0, 1, 2, \ldots, L_2 - 1$.

$\bar{G}^1$ and $\bar{G}^2$ will be used in (7) to replace G when the lattice of squares is one-dimensional and two-dimensional respectively.

3. Application to the study of earthquakes

We now attempt to apply the model of section 2 to the study of earthquakes. The main steps for this are:

(1) Initially, set the stresses on all units to zero.

(2) Initially, assign random numbers between θ_l and 1.0 to the stress thresholds (σ_{th}) of the units (to simulate the heterogeneities of the earth's crust). The random distribution of stress thresholds will be taken as uniform.

(3) Drive the system, i.e. increase the stresses uniformly, until on a unit the stress exceeds the stress threshold (this is called a rupture). An earthquake sequence thus begins after a usually long stress build-up period (tectonic time scale).

(4) Reset† the stress threshold of the ruptured unit to a random number between θ_l and 1.0 (rule I) or to the constant value 1.0 (rule II).

(5) Calculate the stress redistribution [using (7)].

(6) Check if other ruptures occur on the lattice afterwards. If so, then step 4 is repeated for all the ruptured units.

(7) Repeat step 5 for all the rupture events (independently) and do step 6 again. The earthquake sequence stops when the stress is lower than the stress threshold on all units.

(8) Count the number of units (S) that have ruptured during the earthquake sequence. S is a measure of the magnitude of the earthquake, which is assumed to happen instantaneously at the tectonic time scale. Note that if an element ruptures more than once during the sequence, every occurrence is counted (unless otherwise specified).

(9) Go to step 3 to generate the next earthquake sequence.

In order to let the model reach a stationary state, a large number of earthquake sequences are initially discarded. By generating a sufficient number of subsequent sequences, it can be checked whether the cumulative size–frequency distribution obeys a Gutenberg–Richter power law [24]

$$C(S) \propto S^{-\tau}$$

where $C(S)$ is the fraction of sequences during which S or more squares have ruptured, and τ is the exponent of the power law. (It is, in fact, more common to use the size–frequency distribution rather than the cumulative size–frequency distribution. τ must then be replaced by $\tau + 1$.)

The scaling properties of the model will be investigated by a finite-size-scaling analysis. To do this, we try to fit $C(S)$ via the form

$$C(S, L) = S^{-\tau} g[(S-1)L^{-\nu}] \tag{8}$$

where L is the largest dimension in the lattice, g a scaling function and ν an exponent that expresses how the finite-size effects scale with the size of the system‡. When comparing systems with different parameter values, we also attempt

$$C(S, L) = S^{-\tau} g[(S-1)L^{-\nu}/f(X, \theta_l, \alpha)]. \tag{9}$$

The function f is included to test our hypothesis that if the mesh size for a given system is changed, then some of the parameter values must also be changed. The term $(S-1)$ in the scaling function ensures that $g(0) = 1$, i.e. when scaling, we map the size interval $[1, \infty)$ on $[0, \infty)$.

4. Results

We consider lattices with $L \times L_2$ units, where $L_2 = 1$ (unless specified otherwise). The parameters θ_l, X and α are allowed to vary. Also, the degree of disorder in the distribution of stress thresholds can be changed by using one or the other resetting rules (see step 4 in section 3). Rule I maintains the degree of disorder of the initial distribution of stress thresholds, whereas rule II makes disorder disappear after a small number of earthquake sequences. The latter two cases will be respectively identified as *random* σ_{th} and *constant*

† In earlier versions of the model of Xu *et al* [9, 10], they allowed for static fatigue to simulate fore- and aftershocks, and a gradual annealing of the stress thresholds to simulate the spatial organization of faults. Since we are mainly interested in scaling properties, here we employ only the simplest resetting rules.

‡ Some authors use the scaling form $C(S, L) = L^{-\beta} g(S/L^{\nu})$. The two scaling forms are equivalent if we put $\beta = \nu\tau$.

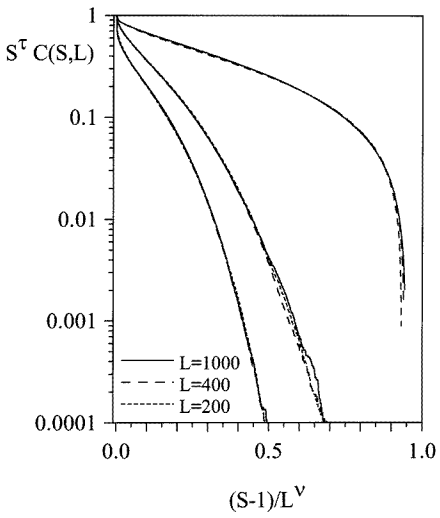

Figure 2. Log–linear scaling plots of the cumulative size–frequency distributions for $L \times 1$ and $L \times 2$ lattices, random σ_{th}, $X = 0$, $\theta_l = 0.25$ and $\alpha = 1$. All curves use the fitting parameter $\tau = 0.30$. For the left and middle curves, all ruptures are counted while for the right curves, only ruptures on distinct units are counted. The left curves were obtained for $L \times 2$ lattices using $\nu = 1.38$, the middle curves for $L \times 1$ lattices using $\nu = 1.38$, and the right curves for $L \times 1$ lattices using $\nu = 1.01$.

σ_{th}. Finally, we let the model reach a stationary state by discarding the first 10^5 earthquake sequences and include 10^6 sequences to do the finite-size-scaling analysis.

4.1. Conservative case ($\alpha = 1$)

We show in figure 1 $C(S, L)$ for random σ_{th}. The main features are the power-law behaviour for small events, and the L-dependent fall-off of the frequency of large events. The power-law behaviour extends over two or three decades. In figure 2, we note that the data sets of figure 1 obey quite well the scaling behaviour predicted by (8) (see the middle curves). The exponent $\tau = 0.30$ was found and cannot be changed by more than 0.01 before there is a noticeable deterioration in the data collapse. As can be seen from figure 1, this value of τ is smaller than the one obtained from a linear fit to the straight segment of the log–log plot (especially for $L = 200$ and $L = 400$). However, the exponent τ is the same if we count the number of ruptures on distinct units or if we count all ruptures. The exponent ν, on the other hand, is different in these two cases, as is the scaling function g. When all ruptures are counted, the same exponents are found for the $L \times 1$ and $L \times 2$ lattices, but the scaling functions are different. We attempted a data collapse of the data sets for $L \times 1$ and $L \times 2$ lattices (when all ruptures are counted) by rescaling the horizontal axis for one of the sets, but found it to be significantly worse than that of figure 2.

We now turn to the effect of having constant stress thresholds. From figure 3, we see that large events become less common. We were unable to find a scaling function which fits both small and large events for $L \times 1$ lattices, no matter if all ruptures or only ruptures on distinct units (results not shown) are counted. However, from figure 3, it is clear that the *shoulder* broadens as L increases, so $C(S, L)$ might scale with L if the small events ($S < 50$) are not considered in the data collapse. We found that, for $\tau = 0.30$ and $\nu = 1.38$ (values obtained above with $L \times 1$ systems having random σ_{th}), the scaling function (8) works well with systems having constant σ_{th} when only the events with $S > 50$ are included in the fit (results not shown). This shows in particular that exponent $\tau = 0.30$ is universal in the sense that it is independent of the degree of disorder in the model. On the other hand, the *crossover* region ($S < 50$) on figure 3 is not a universal feature since it appears only for systems with constant σ_{th}. We have checked that the crossover region is a robust

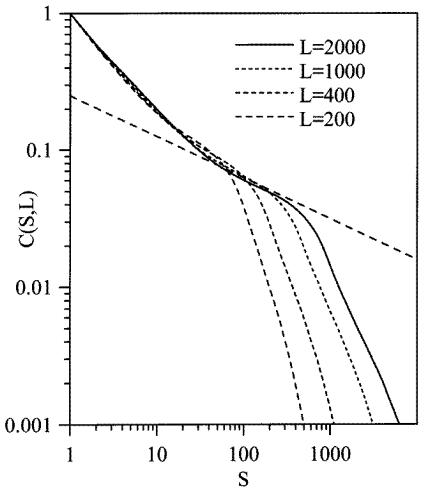

Figure 3. Log–log plot of the cumulative size–frequency distributions for $L \times 1$ lattices, constant σ_{th}, $X = 0$, $\theta_l = 0.25$ and $\alpha = 1$. $S < 50$ is a crossover region and its origin is explained in the text. It is of interest to note that beyond $S > 50$, $C(S, L)$ has a linear segment having a slope close to 0.30. The linear segment beyond $S > 50$ gets longer as L increases but cuts off at large S. For comparison, we show a curve proportional to $S^{-0.30}$.

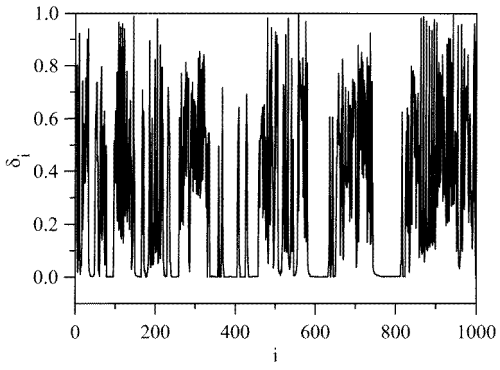

Figure 4. Distribution of the stress differences δ_i between nearest-neighbour elements of a 1000×1 system with constant σ_{th}, $X = 0$, $\theta_l = 0.25$ and $\alpha = 1$. Patches of various sizes are clearly seen for small δ_i ($i = 1, 2, \ldots, 999$). Focusing on the δ_i's smaller than 0.01, then the two biggest patches have sizes 61 (around $i \approx 800$) and 46 (around $i \approx 600$), so the total number of elements at about the same stress level is 62 and 47 in these two cases respectively.

feature which is not sensitive to the initial configuration of the model. Therefore, even if an ensemble average of initial configurations is carried out (see [11]), the crossover region remains.

To explain the presence of the crossover region on figure 3, we calculated the stress differences between nearest-neighbour elements in a system with constant σ_{th}, i.e. $\delta_i \equiv |\sigma_{i+1} - \sigma_i|$ ($i = 1, 2, \ldots, L - 1$ for an $L \times 1$ system). Quantity δ_i was used by Grassberger [25] in a study of the short-range model in [13]. The δ_i's for a 1000×1 system with constant σ_{th} are plotted in figure 4. In this figure, we observe a series of patches of various sizes at small δ_i. In particular, the two biggest patches have sizes 61 and 46, which means that the number of elements at about the same stress level is 62 and 47 in these two cases respectively. Assemblies of elements next to one another, which are at the same stress level, will be referred to as *groups* of elements hereafter. As long as one element in a group has its stress over σ_{th}, then the other elements in the group will *likely* rupture in the same sequence. We have checked that the groups of elements are not static features, i.e. they do not in general involve the same elements at later times. Now, our explanation for the presence of the crossover region ($S < 50$) in figure 3 goes like this: during an earthquake sequence, when the broken elements are found mostly in a given group of elements or in a couple of small groups of elements away from other groups in the system, then the size of the sequence (S) is limited by the number of elements in the group(s), so S tends to be

small (i.e. in the crossover region). In constrast, if broken elements are found mostly in groups of appreciable sizes close to one another, then S tends to be large. In summary, the localized (versus delocalized) nature of the activity in a sequence determines whether S is small or large. This explanation is plausible considering the fact that we have noticed that, for a 1000×2 system with constant σ_{th}, no crossover region is observed since the presence of a second strip of elements allows the delocalization of the activity to take place. Along the same line, systems with random σ_{th} never display patches such as the ones in figure 4, so the localization of the activity never happens. This explains why systems with random σ_{th} always display simple cumulative size–frequency distributions (see figure 1).

We next investigate the effect of the parameter X controlling the fraction of stress retained by a broken unit. The data collapses in figure 5 are seen to be quite good for systems with random σ_{th}. Also, for a fixed L, an increase in X extends the power law to larger S. This makes sense because a larger X means that a ruptured element will retain more stress, so it will be easier to have it involved in the near future in an earthquake sequence (because stress remains close to stress threshold). As a result, the largest size for an earthquake sequence increases. In figure 6, we show, for a 1000×1 lattice and random σ_{th}, a fit to the scaling form

$$C(S, L) = S^{-\tau} g[(S-1)L^{-\nu}/f(X)].$$

The fit, although not perfect, implies that a system which has been discretized by a fine mesh and a small value of X (i.e. a ruptured unit almost opens) can be approximated by a coarser mesh and a larger value of X (i.e a smaller fraction of the stress is released by the ruptured unit).

The effect of changing the lower bound θ_l for the stress threshold distribution is shown in figure 7. The data collapses are very good for systems with random σ_{th}. For a fixed L, a decrease in θ_l extends the power law to larger S. Comparing figures 5 and 7, we see that, for a given L, an increase in X has much the same effect on $C(S, L)$ as a decrease in θ_l.

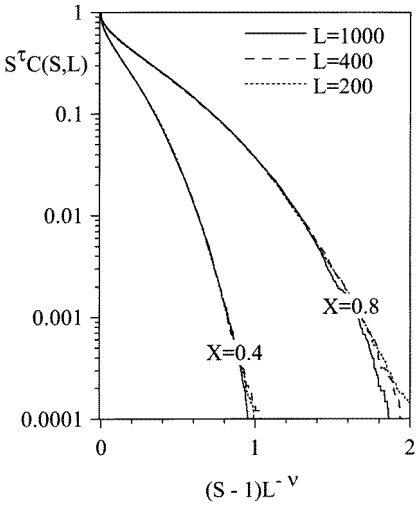

Figure 5. Log–linear scaling plots of the cumulative size–frequency distributions for $L \times 1$ lattices, random σ_{th}, $\theta_l = 0.25$, $\alpha = 1$ and two values of X. Exponents used are $\tau = 0.30$ and $\nu = 1.38$.

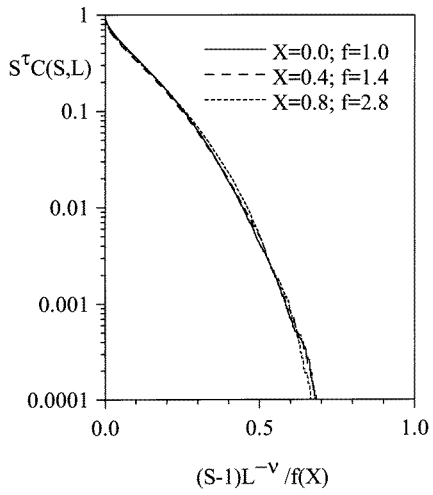

Figure 6. Log–linear scaling plot of the cumulative size–frequency distributions for a 1000×1 lattice, random σ_{th}, $\theta_l = 0.25$, $\alpha = 1$ and three values of X. Exponents used are $\tau = 0.30$ and $\nu = 1.38$.

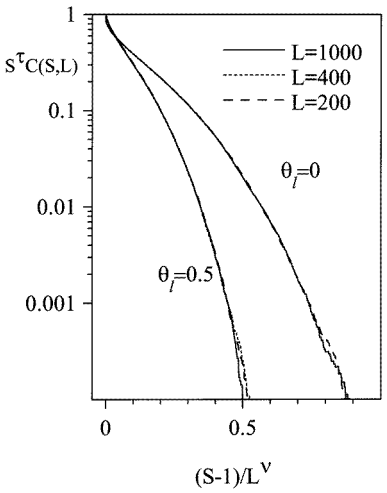

Figure 7. Log–linear scaling plots of the cumulative size–frequency distributions for $L \times 1$ lattices, random σ_{th}, $X = 0$, $\alpha = 1$ and two values of θ_l. Exponents used are $\tau = 0.30$ and $\nu = 1.38$.

We have also attempted a fit to the scaling form

$$C(S, L) = S^{-\tau} g[(S-1)L^{-\nu}/f(\theta_l)].$$

The quality of the fit is very similar to the one in figure 6 and is therefore not shown. We obtain a reasonable fit for a 1000×1 lattice and random σ_{th} using $\tau = 0.30$ and $\nu = 1.38$. If we choose $f(\theta_l) = 1$ for $\theta_l = 0.5$, we find $f(\theta_l) = 1.32$ for $\theta_l = 0.25$ and $f(\theta_l) = 1.64$ for $\theta_l = 0.0$. This result implies that a system which has been discretized by a fine mesh and a large value of θ_l, can be approximated by a coarser mesh using a smaller value of θ_l. We expect that this near equivalence can be made even better if we simultaneously adjust both X and θ_l.

We have also investigated the effects of changing X and θ_l in systems with constant σ_{th}. Again, we fail to find a satisfactory scaling form which is valid for both small and large events since a crossover region at small S is still present. As we did above, we attempted data collapses for various X and θ_l by focusing only on the events outside the crossover region and found that with $\tau = 0.30$ and $\nu = 1.38$, the scaling function (8) works well. This shows once more that $\tau = 0.30$ is a universal value.

Before we consider the case of non-conservative systems ($\alpha < 1$), we comment on the value obtained for exponent τ. We have obtained through a finite-size-scaling analysis $\tau = 0.30 \pm 0.01$, which seems to be robust. This value can be compared with that in [26] (0.31 ± 0.04), which was obtained with a long-range scalar model with quenched disorder (stress thresholds are kept equal to their initial random values throughout a simulation). Our value of τ is in agreement with the latter, but is not in agreement with the value (0.4) obtained by Xu *et al* [10] and Chen *et al* [8] for a two-dimensional system. However, their value was determined approximately from a linear fit to the straight segment of the log–log plot and not by a finite-size-scaling analysis, and so the comparison is not conclusive. Finally, Christensen and Olami [27] obtained a different value (0.22 ± 0.05) through a finite-size-scaling analysis of a short-range, two-dimensional model with constant σ_{th} [13]. Therefore, the models in [13] and [10] seem to belong to different universality classes.

4.2. Non-conservative case ($\alpha < 1$)

In this section, we examine two effects for $L \times 1$ systems with random σ_{th} and constant σ_{th} when X is fixed to 0 and θ_l to 0.25. The first one is the effect of parameter α for fixed L,

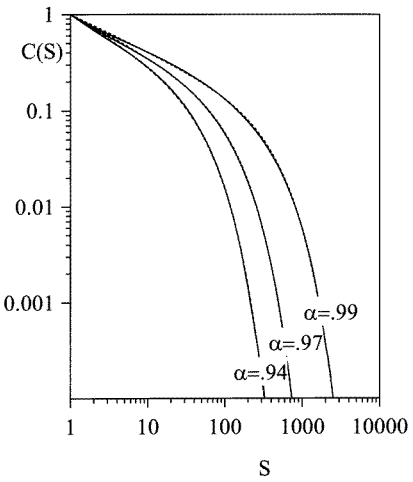

Figure 8. Log–log plot of the cumulative size–frequency distributions for a 2000×1 lattice, random σ_{th}, $X = 0$, $\theta_l = 0.25$ and three values of α.

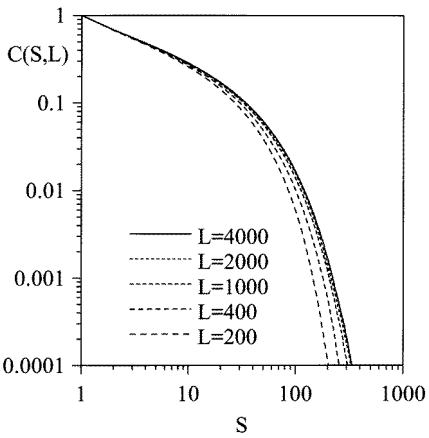

Figure 9. Log–log plot of the cumulative size–frequency distributions for $L \times 1$ lattices, random σ_{th}, $X = 0$, $\theta_l = 0.25$ and $\alpha = 0.94$.

and the second is the effect of L for a fixed $\alpha < 1$.

In figure 8, we present cumulative size–frequency distributions for different values of the parameter α controlling the level of stress nonconservation (or dissipation). It can be seen on figure 8 for a 2000×1 lattice with random σ_{th} that a decrease in α makes the power law cut-off happens at increasingly smaller S. Also, as α decreases, the slope of the straight segment of the log-log plot increases, an effect which was also noticed in [27].

In figure 9, we show $C(S, L)$ for $\alpha = 0.94$, random σ_{th} and different lattice sizes (L). As expected, as L increases, the straight segment of the log–log plot extends to larger S. However, a saturation is noticed for $L = 2000$–4000. We have attempted to fit the cumulative size–frequency distribution for fixed L (and α) to

$$C(S) = S^{-\tau} \exp[(1 - S)/S_0 + bS^2 + cS^3 + \cdots]. \tag{10}$$

For large L, we found that only the first term in the argument of the exponential is significant, where S_0 is a characteristic earthquake size. In this case, (10) reduces to a form similar to that used in [14]. In table 1, the values of τ and S_0 are given for various values of α and L. For a fixed α, S_0 increases with L and appears to saturate, but certainly $S_0(L)$ diverges much slower than L ($S_0(L) \sim L^{\beta}$ with $\beta \ll 1$). A similar conclusion was drawn by Jánosi and Kertész [28] in a study of a version of the short-range model in [13], possibly with a different value of β. From table 1, we also note that, for a fixed L, S_0 increases with α and τ increases as α decreases. We therefore corroborate quantitatively conclusions obtained qualitatively from the curves in figure 8.

We have examined the above two effects for systems with constant σ_{th} as well. The results obtained are not shown since the conclusions that can be drawn from them are identical to those obtained for systems with random σ_{th}. Again, as in the conservative case, a crossover region is still observed. Then, a straight line can be fitted for fixed L and α to the log–log plot of $C(S, L)$ for values of S outside the crossover region (up to a cut-off value much smaller than in the conservative case). We noted that the slope of the straight segment increases and the cut-off value decreases as α decreases. Also, for a fixed α, we found that the cut-off value saturates as L increases. Because the cut-off value for fixed L

Table 1. Exponent τ and characteristic earthquake size S_0 for $L \times 1$ lattices, random σ_{th}, $X = 0$, $\theta_l = 0.25$ and three values of α.

α	L	τ	S_0
0.94	4000	0.482	52.2
0.94	2000	0.477	50.0
0.94	1000	0.490	48.2
0.94	400	0.419	37.2
0.94	200	0.354	27.4
0.97	2000	0.428	115
0.97	1000	0.405	98.5
0.97	400	0.361	70.6
0.99	2000	0.386	407
0.99	1000	0.367	307
0.99	400	0.277	149

and $\alpha < 1$ is smaller than in the case $\alpha = 1$, we can again associate a characteristic size S_0 to $C(S, L)$ [see (10)]. The saturation of the cut-off value as L increases and the fact that $S_0(L)$ diverges much slower than L are therefore expressing the same idea.

Finally, it was observed that simulations running for longer times are providing data which are not altering our results. This is in contrast to a study of the short-range model in [13], which found that the time for total invasion of the interior of large lattices by SOC can be very large, especially for values of α close to 0.0 [29]. We believe that because the model of Xu *et al* is long-range, invasion is much faster than in the model in [13]. This therefore confirms the above observation.

5. Summary and conclusions

We have studied a version of an earthquake model introduced by Xu *et al* in which only one shear mode of rupture can occur. A new ingredient was added to the model by coarse-graining the lattice Green function used in the computation of stress redistribution upon rupture. The conclusions that can be drawn from our study involving one-dimensional ($L \times 1$) systems are the following: the finite-size-scaling function (8) works well over the whole range of S in the presence of disorder and for S larger than about 50 in the absence of disorder. In the absence of disorder, there is a crossover region for $S < 50$ and it appears whatever the parameter values. The existence of such a crossover region is related to the localized nature of the activity on a group of elements or on a couple of small groups of elements at about the same stress level isolated from any other group in the system. The crossover region disappears for two-dimensional systems in the absence of disorder and as soon as disorder is present in a system (both one-dimensional and two-dimensional).

The effects of parameters X and θ_l were also investigated and we found a fair agreement with the finite-size-scaling function (9) over the whole range of S in the presence of disorder and for S larger than about 50 (outside the crossover region) in the absence of disorder. We noticed also that an increase in the parameter X (parameter controlling the degree of stress retained by a ruptured unit) has roughly the same effects on the cumulative size–frequency distributions as a decrease in θ_l (parameter controlling the width of the uniform distribution of stress thresholds).

The exponents of the finite-size-scaling functions (8) and (9) were found to be $\tau = 0.30 \pm 0.01$ and $\nu \approx 1.38$. This value of τ is robust and in particular, it is independent

of the degree of disorder in the system.

Introduction of stress nonconservation (controlled by parameter α) results in the appearance of a characteristic earthquake size (S_0), which is smaller than L for large L. However, at least for α close to unity, it is possible that $S_0(L)$ diverges as L^β with $\beta \ll 1$. A similar conclusion was drawn by Jánosi and Kertész [28] (probably with a different value of the exponent). For a fixed L, S_0 increases with α and the exponent τ increases as α decreases. The latter observation is in agreement with the findings of Christensen and Olami [27]. The conclusions drawn from our results were found to be independent of the degree of disorder in the system.

In the future, we plan to present an analysis of the time series obtained from the model (e.g. earthquake size and average stress in the system as a function of tectonic time).

Acknowledgments

BB and HJX are grateful to Kan Chen and Chao Tang for teaching them about self-organized criticality (SOC) and for many helpful suggestions over the years. DG acknowledges the financial support from Le Fonds FCAR of the government of Québec. This work was also supported by the Natural Sciences and Engineering Research Council of Canada. This paper has greatly benefited from the review by an unknown referee.

References

[1] Bak P, Tang C and Wiesenfeld K 1987 *Phys. Rev. Lett.* **59** 381
[2] Sornette D, Johansen A and Dornic I 1995 *J. Physique* I **5** 325
[3] Bak P and Tang C 1989 *J. Geophys. Res.* B **94** 15, 635
[4] Sornette A and Sornette D 1989 *Europhys. Lett.* **9** 197
[5] Bak P and Chen K 1991 *Fractals and Their Application to Geology* ed C C Barton and P R LaPointe (Denver, CO: Geological Society of America)
[6] Burridge R and Knopoff L 1967 *Bull. Seism. Soc. Am.* **57** 341
[7] Mora P and Place D 1993 *Int. J. Mod. Phys.* C **4** 1059
[8] Chen K, Bak P and Obukhov S P 1991 *Phys. Rev.* A **43** 625
[9] Xu H-J, Bergersen B and Chen K 1992 *J. Phys. A: Math. Gen.* **25** L1251
[10] Xu H-J, Bergersen B and Chen K 1993 *J. Physique* I **3** 2029
[11] Herrmann H J and Roux S (ed) 1990 *Statistical Models for the Fracture of Disordered Media* (Amsterdam: North-Holland)
[12] Burridge R and Knopoff L 1964 *Bull. Seism. Soc. Am.* **54** 1875
[13] Olami Z, Feder H J S and Christensen K 1992 *Phys. Rev. Lett.* **68** 1244
[14] Lise L and Jensen J H 1996 *Phys. Rev. Lett.* **76** 2326
[15] Bottani S 1995 *Phys. Rev. Lett.* **74** 4189
[16] Corral Á, Pérez C J, Díaz-Guilera A and Arenas A 1995 *Phys. Rev. Lett.* **75** 3697
[17] Weibull W 1951 *J. Appl. Mech.* **8** 293
[18] Love A E H 1944 *A Treatise on the Mathematical Theory of Elasticity* (New York: Dover)
[19] Bhagavatula R, Chen K and Jayaprakash C 1994 *J. Phys. A: Math. Gen.* **27** L155
[20] Grinstein G, Lee D-H and Sachdev S 1990 *Phys. Rev. Lett.* **64** 1927
Hwa T and Kardar M 1989 *Phys. Rev. Lett.* **62** 1813
[21] Drossel B and Schwabl F 1992 *Phys. Rev. Lett.* **69** 1629
[22] Bak P and Sneppen K 1993 *Phys. Rev. Lett.* **71** 4083
[23] Gabrielov A, Newman W I and Knopoff L 1994 Phys. Rev. E **50** 188
[24] Gutenberg B and Richter C F 1944 *Bull. Seism. Soc. Am.* **34** 185
[25] Grassberger P 1994 *Phys. Rev.* E **49** 2436
[26] Miltenberger P, Sornette D and Vanneste C 1993 *Phys. Rev. Lett.* **71** 3604
[27] Christensen K and Olami Z 1992 *Phys. Rev.* A **46** 1829
[28] Jánosi I M and Kertész J 1993 *Physica* **200A** 179
[29] Middleton A A and Tang C 1995 *Phys. Rev. Lett.* **74** 742